RSC Advances

ROYAL SOCIETY OF CHEMISTRY

www.rsc.org/advances

Journal Name

RSCPublishing

ARTICLE

Effect of Migration of Layered Nanoparticles during Melt Blending on Phase Morphology of Poly (ethylene terephthalate)/Polyamide 6/ Montmorillonite Ternary Nanocomposites

Guomin Xu[a,b], Shuhao Qin [b], Jie Yu [b], Yifu Huang [a], Mingqiu Zhang [a], Wenhong Ruan [a *]

To study the effect of migration and selective localization of layered nanoparticles during melt compounding on phase morphology of polymer blends, poly (ethylene terephthalate) (PET)/polyamide 6 (PA6)/organic montmorillonite (OMMT) ternary nanocomposites were prepared. Three different blending sequences were adopted either by pre-compounding OMMT into PET or into PA6 or by mixing all three components together. Morphology and tensile properties of PET/PA6/OMMT nanocomposites were investigated. TEM observation showed that OMMT platelets exclusively localized within PA6 phase independent of the blending sequences, suggesting OMMT platelets migrated from PET into PA6 phase during both one-step and two-step compounding process with pre-mixed PET/OMMT, and this migration was attributed to the interfacial effects. SEM results revealed that the migration and selective localization of OMMT platelets had great influence on the size of dispersed phase due to the conjunct action of migration cutting effect and viscosity effect. And the morphology determines the final properties of the nanocomposites as indicated by tensile test. It is believed that this work provides a way to tune the morphology and performance of immiscible blends.

1 Introduction

In recent years, the addition of layered nanoparticles, such as nanoclay and graphene, into immiscible polymer blends has generated much interest owing to the possibility of combining the advantage of the blends with the nano-effect of the nanoparticles. It can further improve the performance of the blends and endow the nanocomposites with functional features [1-6]. Studies showed that the addition of layered nanoparticles has great effects on the microstructure of the nanocomposites, which can be represented by the size, shape, and homogeneity of the morphology [7], and the microstructure in turn determines the performance of the nanocomposites [8]. In fact, microstructure of the nanocomposites is one of the common issues that researchers focused on.

As a kind of commercial nanoparticles, layered montmorillonite (OMMT) has been widely studied to prepare nanocomposites [5-12]. It is found that OMMT could be exclusively distributed in one phase or existed at the interface of immiscible polymer blends, and this selective localization has a great influence on the phase morphology of the blends [9-12]. The recent research reported by Soulestin et al. found that in poly (ethylene terephthalate) (PET)/ polyethylene (PE) (80/20) system, most OMMT platelets localized in PET matrix and few platelets localized at the interface of PET/PE. The selective localization of OMMT in PET matrix decreased the size of PE dispersed phase [9]. While the research of Ghasemi et al. found that the preferential localization of nanoclays in PC dispersed phase of polycarbonate (PC)/polybutylene terephthalate (PBT) (30/70) system also decreased the size of dispersed phase [10]. In our previous studies, we also found that in acrylonitrile butadiene styrene (ABS)/ polyamide 6 (PA6) (70/30) system the selective localization of nanoclays in the PA6 dispersed phase greatly reduced the size of dispersed phase [11]. However, in poly (methyl methacrylate) (PMMA)/high-density polyethylene (HDPE) (30/70) blend, it is observed that the preferential localization of nanoclays into PMMA dispersed domains conversely increased the size of PMMA dispersed phase [12].

In addition, the selective localization of OMMT had a great influence on the performance of the nanocomposites [13-15]. It was reported that localization of nanoclay particles in matrix phase resulted in the increase of tensile modulus more efficiently than those localized in dispersed phase [14]. While Motamedi etc. observed that the localization of nanoclay within PA6 dispersed phase enhanced the stiffness and toughness of PP/PA6 nanocomposites [15].

Based on the above analysis, it is noteworthy that there is still no consistent conclusion in the effect of selective localization of OMMT on the morphology and performance of the blends. Although the selective localization of OMMT in the polymer blends was demonstrated, the effect of migration of OMMT from one phase to another phase on the microstructure of the blends during melt compounding was rarely concerned. Moreover the relevant mechanism was not elucidated thoroughly. Indeed, the effects of OMMT on phase morphology of blends are complicated, which depends on the components and the processing of the blends. Therefore, a further investigation on the migration of OMMT in polymer blends and the effect on phase morphology are still needed.

In order to systematically study the effect of migration and selective localization of layered nanoparticles on the morphology of immiscible blends, OMMT was chosen as representative layered nanoparticles to incorporate into the typical immiscible blends of PET/PA6. The blends of PET/ PA6 are of interest in the area of food packaging because of their potential for combining the low oxygen and carbon dioxide permeability of polyamides with the good toughness, clarity, and economics of the polyester [16]. To demonstrate the migration of OMMT in polymer blends during melt compounding, three different blending sequences were carefully designed comparatively. Furthermore, the size of dispersed phase of the blends as a function of OMMT content and PET/PA6 composition was investigated and discussed. We hope that this work can give a way of tuning the morphology and performance of immiscible blends.

2 Experimental

2.1 Materials

PET pellets (SBG801) were purchased from Far Eastern Industries (Shanghai) Ltd, with a density of 1.4g/cm^3, an intrinsic viscosity of 0.79dL/g at 30^{o}C, a melting point of 243^{o}C, and a glass transition temperature of 77^{o}C. PA6 (1030B) was a commercially available product from Ube Co. Japan, with a weight-average molecular weight of 30000g/mol, a density of 1.14g/cm^3, a melting point of 220^{o}C, and a glass transition temperature of 67^{o}C. OMMT (DK2) modified by methyl tallow bis (2-hydroxyethyl) ammonium with the cation exchange capacity of 120meq/100g was supplied by Zhejiang Feng Hong Clay Co. Ltd., (ANJI Zhejiang, China). Each structure of the materials (PET, PA6 and modified OMMT) is shown in Fig.1, respectively.

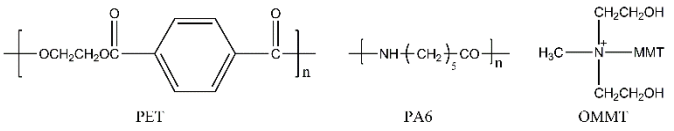

Fig.1 Structure of the materials (PET, PA6 and modified OMMT)

2.2 Nanocomposites preparation

Before melt blending, PA6 pellets and OMMT were dried in a vacuum oven at 80^{o}C for 24h and PET were dried at 130^{o}C for 4h to reduce the moisture-induced thermal degradation during compounding. To investigate the effect of migration and selective localization of OMMT on the final phase morphology and microstructure, three different blending sequences were employed: direct blending of all components in one processing step (one-step compounding) or blending of pre-mixed PA6/OMMT or pre-mixed PET/OMMT with the respective unfilled polymer (PET or PA6) in a second step (two-step compounding). Firstly, all the blends of PET/PA6 and the nanocomposites of PET/PA6/OMMT were prepared by a twin-screw co-rotating extruder (L/D=40, D=20mm, Coperion Keya (Nanjing, China) Machinery Co. Ltd.), with the temperature program of 220, 245, 255, 250, 245, 245^{o}C and the screw speed of 320rpm/min. The proportion of PET/PA6 in the resulting products was kept at either 70/30 or 30/70. Finally, all the blends and nanocomposites were injection molded (Type CJ80M3V, Chen De Plastics Machinery Co.Ltd., Guangdong, China) at 255^{o}C with a cooling time of 15s into various specimens for morphological observation and characterization.

2.3 Characterization

The distribution and selective localization of OMMT in the PET/PA6 blends were observed by JEM-200CX transmission electron microscopy (TEM) (JEOL Ltd., Japan) at an accelerating voltage of 120kV. Ultrathin sections with the thickness of 60-80nm were cut from Izod bars perpendicular to the flow direction under cryogenic conditions using a LKB-5 microtome (LKB Co, Switzerland).

Contact angle measurement was taken at room temperature by using sessile drop method on the dynamic surface analyzer (DSA 100, Kruss, Germany). The contact angles of neat PET and PA6 were measured. Surface tension of the polymers was calculated by using the Young's equation:

$$\gamma_{SL} + \gamma_{LV}\cos\theta = \gamma_{SV} \quad (1)$$

Where γ_{SL}, γ_{LV}, and γ_{SV} represent the interfacial energy of the solid/liquid, liquid/air, solid/air interface, respectively, and θ is the contact angle between the liquid and the solid surface.

The phase morphology of PET/PA6 blends and PET/PA6/OMMT nanocomposites was observed with a KYKY-2800 scanning electron microscope (SEM, KYKY Technology Development Ltd., China) at an accelerating voltage of 25kV. The sample surface for SEM observation was prepared as follows: firstly, the samples were carefully immersed in liquid nitrogen and quickly brittle-fractured; then the PA6 dispersed phase on the fractured surface of samples was etched with formic acid for 2h, or the PET dispersed phase

on the fractured surface was etched with 10% KOH ethanol solution for 4h; the sample surface was thoroughly washed with deionized water and vacuum-dried at room-temperature; lastly, the etched surface of the specimens was gold sputtered for observation.

To quantitatively analyze the morphology of the fractured surface of the sample, the number-average domain diameters (D_n) were obtained by using the following equation:

$$D_n = \sum \frac{D_i}{N} \qquad (2)$$

Where N is the total number of dispersed domains, D_i is the particle diameter of a domain. More than 200 particles were analyzed for the accuracy of statistical samplings.

The rheological properties in frequency sweep mode of neat PA6, PET, and PA6/OMMT nanocomposites with different OMMT contents were measured at 255°C by an advanced rheometrics expansion system (AR-1000, TA Instruments, Inc., New Castle, Delaware) with Φ25mm parallel plates and plate separation of 2mm. The strain sweeps were first performed before dynamic test to ensure that the frequency sweeps were within the linear viscoelastic and stable region. In this test, the strain amplitude was 1%.

The tensile properties of the nanocomposites were carried out by using a universal tensing machine (CMT6104, Shenzhen XINSANSI Co. Ltd., China) according to the China national standard (GB 1040.2-2006), at a cross-head speed of 50mm/min, at ambient conditions. The fracture strength was used to determine the tensile strength, and a minimum of five specimens were tested to achieve average value.

3 Results and discussion

3.1 Distribution of OMMT in nanocomposites

Fig.2 showed TEM micrographs of PET/PA6/OMMT (70/30/3) and PET/PA6/OMMT (30/70/3) prepared by different compounding sequences. It can be seen that PET domains (light region) and PA6 domains (dark region) in the immiscible PET/PA6 blends can be clearly distinguished under TEM observation without using a phase-contrast staining treatment. From TEM micrographs of nanocomposites prepared by two-step compounding with pre-mixed PET/OMMT (Fig.2(a) and (b)), it is surprising to see that majority of OMMT nanoplatelets localized in PA6 phase, demonstrating the migration of OMMT platelets from PET phase to PA6 phase during melt blending. Fig.2 (c) and (d) showed that OMMT platelets (dark lines or platelets) exclusively localized in PA6 phase when blended PET/PA6/OMMT simultaneously by one-step compounding, indicating OMMT platelets also migrated and selectively localized in PA6 phase. While for nanocomposites with pre-mixed PA6/OMMT, most OMMT platelets stayed in PA6 phase (Fig.2 (e) and (f)), indicating non-migration of OMMT platelets in these systems. Interestingly, most of the dispersed phases are elliptical in appearance and the TEM observations clearly revealed that the OMMT platelets were exclusively located within the PA6 phase in all blends, regardless of the way of introducing the OMMT.

It is known that the wetting coefficient (ω_a) can predict the selective distribution of nanoparticles in those immiscible polymer blends with thermodynamic reason [15,17]. It can be calculated by Young's equation:

$$\omega_a = \frac{\gamma_{OMMT\text{-}PA6} - \gamma_{OMMT\text{-}PET}}{\gamma_{PA6\text{-}PET}} \qquad (3)$$

where $\gamma_{OMMT\text{-}PA6}$, $\gamma_{OMMT\text{-}PET}$ and $\gamma_{PA6\text{-}PET}$ are the interfacial tensions between OMMT-PA6, OMMT-PET, and PA6-PET respectively. If the ω_a is higher than 1, the OMMT platelets will localize in PET, if the ω_a is lower than −1, it will preferentially distribute in PA6, and if the ω_a is between 1 and −1, the OMMT platelets will localize at the interface between the two phases.

The interfacial tensions between pairs of components according to the geometric mean and harmonic mean equations

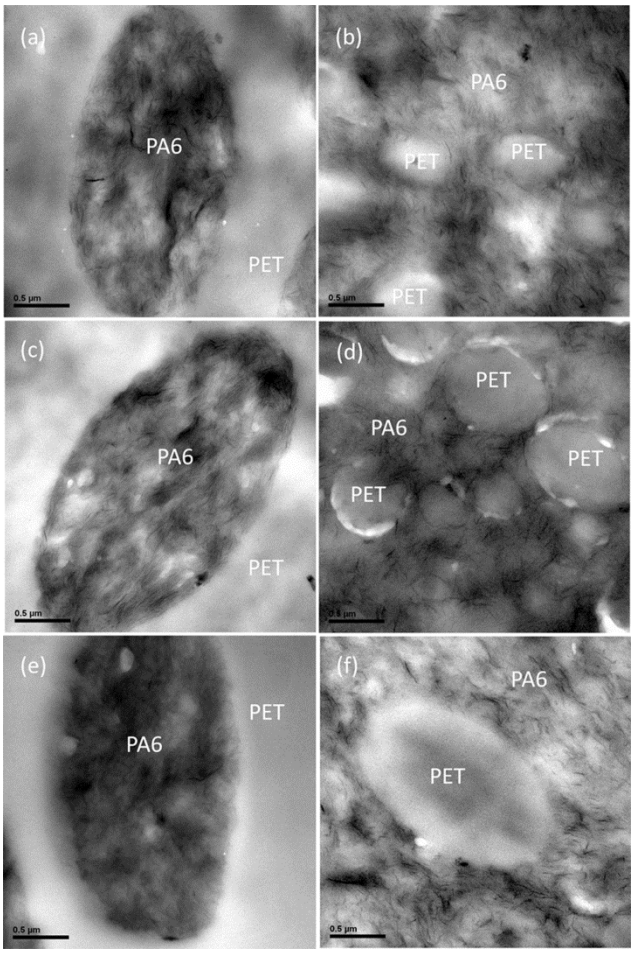

Fig.2 TEM micrographs of nanocomposites prepared by different melt blending sequences: (a) PET/PA6/OMMT (70/30/3) and (b) PET/PA6/OMMT (30/70/3) by two-step compounding with pre-mixed PET/OMMT. (c) PET/PA6/OMMT (70/30/3) and (d) PET/PA6/OMMT (30/70/3) by one-step compounding. (e) PET/PA6/OMMT (70/30/3) and (f) PET/PA6/OMMT (30/70/3) by two-step compounding with pre-mixed PA6/OMMT

were calculated (see supporting information in Table 1S) and summarized in Table 1. Then ω_a could be obtained according to Eq.(1). Because of the ω_a<-1, these calculations provide an explanation of selective distribution of OMMT in the PA6 phase by interfacial effects. Consequently, the migration of OMMT from PET phase into PA6 phase when thermodynamic equilibrium had been theoretically proved.

Table.1 Interfacial tensions and wetting coefficients according to geometric and harmonic mean equations

Material	Interfacial tension, mN/m		Wetting coefficient, ω_a		Location prediction
	Geometric mean equation	Harmonic mean equation	Geometric mean equation	Harmonic mean equation	
PET/PA6/OMMT	γ_{12}= 0.99 γ_{13}=0.96 γ_{23}=2.54	γ_{12}= 2.42 γ_{13}= 1.83 γ_{23}= 5.34	-1.61	-1.60	PA6

Note: 1-PA6, 2-PET, 3-OMMT

3.2 Phase morphology of PET/PA6/OMMT nanocomposites

To further study the effect of migration and selective localization of OMMT on the phase morphology of PET/PA6/OMMT nanocomposites, the image analyzing software (Image-Pro, Media Cybernetics Inc.) was used to analyze the SEM micrographs. Fig.3 depicts the SEM images of the representative nanocomposites prepared by two-step compounding with pre-mixed PET/OMMT, in which migration of OMMT occurred. It can be seen that the nanocomposites show a typical sea-island morphology, where hollow domains indicate the PA6 dispersed phase extracted by formic acid in PET/PA6 (70/30) systems or the PET dispersed phase extracted by 10% KOH ethanol solution in PET/PA6 (30/70) systems. It also can be seen that the size of spherical dispersed phase changes with the content of OMMT, no matter in PET/PA6 (70/30) (From Fig.3 (a) to (d)) or in PET/PA6 (30/70) systems (From Fig.3 (e) to (h)). On the basis of the SEM images, the plot of the number-average dispersed domain diameter (D_n) versus the amount of OMMT was shown in Fig.4. It is obvious that the D_n of PET/PA6 (70/30) nanocomposites increases with the content of OMMT increased (see line 1 in Fig.4 (a)). While the dispersed phase size decreases as clay content increases in PET/PA6 (30/70) blends (see line 1 in Fig.4 (b)).

Moreover, the D_n versus OMMT amount of the nanocomposites prepared by one-step compounding and two-step compounding with pre-mixed PA6/OMMT were counted as well, and the results were shown in Fig.4 comparatively. It can be seen that in PET/PA6 (70/30) blends (Fig.4 (a)), the D_n of the nanocomposites increase with the content of OMMT monotonically, obviously for those of two-step nanocomposites with pre-mixed PET. While for PET/PA6 (30/70) blends (Fig4 (b)), the trend is not monotonic like that of PET/PA6 (70/30) blends. It is obvious that the D_n of one-step compounding blends and two-step compounding blends with pre-mixed

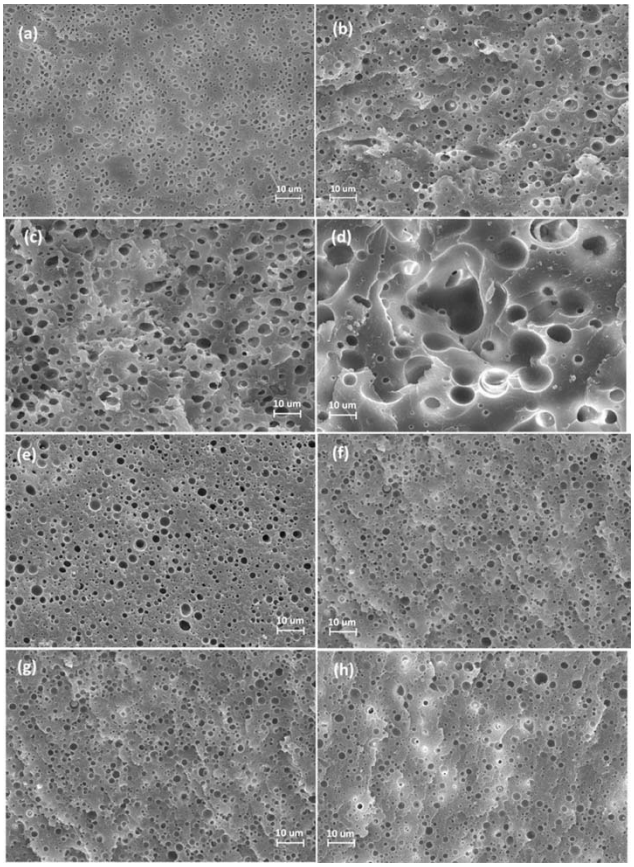

Fig.3 SEM micrographs of PET/PA6/OMMT nanocomposites prepared by two-step sequence with pre-mixed PET/OMMT: (a) 70/30/0, (b) 70/30/1, (c) 70/30/3, (d) 70/30/5, (e) 30/70/0, (f) 30/70/1, (g) 30/70/3, (h) 30/70/5

PET/OMMT decreases as the content of OMMT increased (see line 1 and 2 in Fig.4 (b)). On the contrary, the D_n of two-step compounding blends with pre-mixed PA6/OMMT decreases at low OMMT content and then increases as the OMMT content increased to 5wt% (see line 3 in Fig.4 (b)). It is realized that the migration and selective localization of OMMT have great effect on the morphology of the nanocomposites.

It is known that the ultimate domain size in immiscible blends is determined by the balance between two opposing factors: droplet breakup and coalescence, which are greatly influenced by the phase separation of the polymer melt and the viscosity of matrix and dispersed phase [18-22]. To evaluate the effect of OMMT on the viscosity of matrix phase and dispersed phase, the complex viscosity (η^*) of neat PET, PA6 and PA6/OMMT was measured by rheological measurement and the results were shown in Fig.5. It is obvious that the η^* of PA6/OMMT is higher than that of neat PA6 and neat PET in high frequency range except PA6/OMMT (100/1) component. In addition, the η^* of PA6/OMMT increases with the content of OMMT increased. This means that OMMT would decrease the viscosity of the filled polymer at low loading, and increase the viscosity of polymer when OMMT content increased. In the previous study, it is indicated that the preferential location of clay in matrix phase would increase the viscosity of matrix

phase and act as a barrier to prevent the coalescence of dispersed phase, consequently the size of dispersed phase is reduced. On the other hand, the preferential location of clay in dispersed phase would increase the viscosity and elasticity of dispersed phase, therefore, the size of dispersed phase is increased due to lack of contribution to coalescence prevention [23]. Based on the above analysis, we would infer that the increased viscosity of PA6/OMMT would increase the size of PA6 dispersed phase of PET/PA6 (70/30) systems, and would decrease the size of PET dispersed phase of PET/PA6 (30/70) systems in which PA6 is matrix phase.

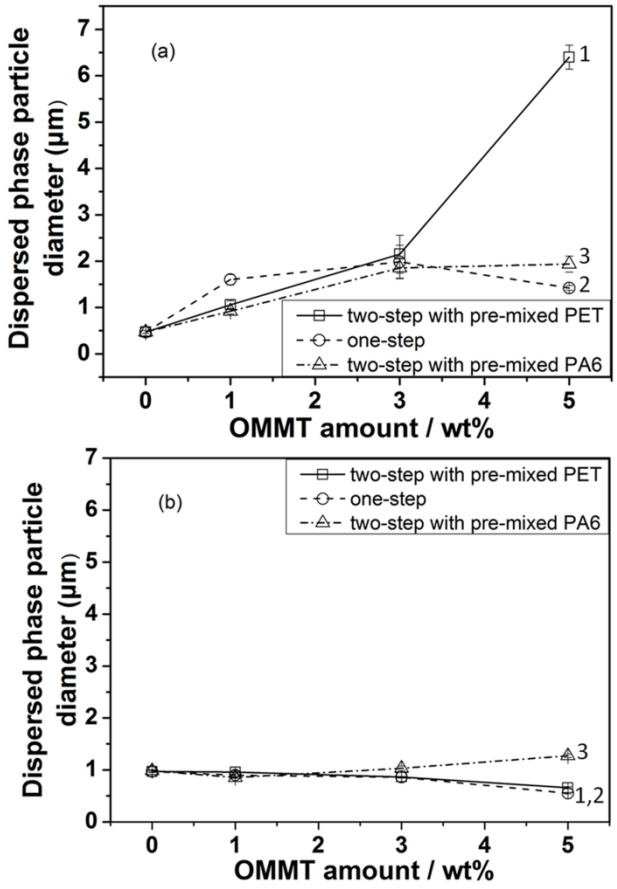

Fig.4 Plots of diameter of the dispersed domain (Dn) of: (a) PET/PA6(70/30) and (b) PET/PA6(30/70) blend prepared by different sequence versus the amount of OMMT.

Moreover, migration of OMMT platelets during melt blending also affected the droplet breakup and coalescence owing to so-called "cutting effect" [24]. It is pointed that OMMT platelets tended to form special "knife-like" structure in the polymer blends. This "clay knife" can split the matrix or dispersed domain apart during migration process under the shear stress, changing the coalescence prevention of the matrix on the dispersed phase.

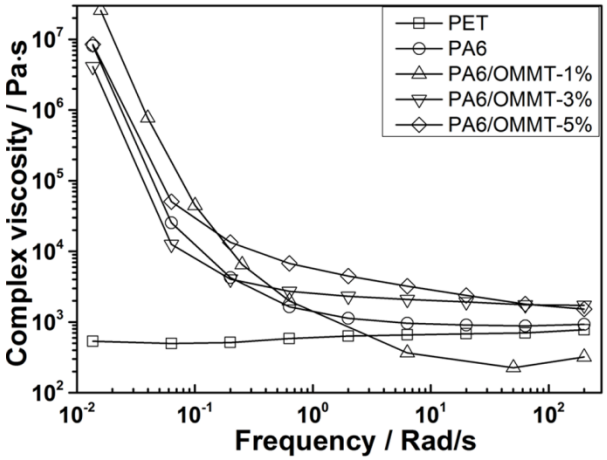

Fig.5 Logarithmic plot of complex viscosity (η^*) of polymers and nanocomposites versus the angular frequency at 255°C

In the melting blending process of PET/PA6/OMMT, it is assumed that viscosity effect and migration cutting effect coexisted. For PET/PA6 (70/30) systems, the dispersed phase is PA6. The selective localization of OMMT in PA6 lead to the viscosity of dispersed phase increase (see Fig.5), which would increase the size of dispersed phase. But the migration effect of OMMT was different in nanocomposites prepared by different compounding sequences. In the nanocomposites prepared by two-step compounding with pre-mixed PET/OMMT, migration of OMMT from PET phase to PA6 phase apparently occurred, which might split the matrix phase of PET and reduce the coalescence prevention of PET on the dispersed phase. Therefore, the size of dispersed phase of PA6 increased greatly with the increase of OMMT content due to the conjunct action of migration cutting effect and viscosity effect (see Fig.3(a)-(d) and line 1 in Fig.4 (a)). While in the nanocomposites prepared by one-step compounding or those prepared by two-step compounding with pre-mixed PA6/OMMT, the cutting effect on the PET matrix greatly decreased because the migration of OMMT from PET to PA6 phase was reduced. As a result, the increase of the size of dispersed phase is less (see line 2 and 3 in Fig.4 (a)).

For the PET/PA6 (30/70) systems, the dispersed phase is PET. The selective localization of OMMT in PA6 leads to the increase of the viscosity of matrix phase (see Fig.5), which would decrease the size of dispersed phase. The migration cutting effect of OMMT from PET to PA6 phase might also decrease the size of dispersed phase as well. Consequently, the size of dispersed phase of PET decreased in the nanocomposites prepared by one-step compounding or two-step compounding with pre-mixed PET/OMMT (see line 1 and 2 in Fig.4 (b)). However, in the non-migration nanocomposites prepared by pre-mixed PA6/OMMT, the size of dispersed phase increased abnormally (see Fig.3 (e)-(h) and line 3 in Fig.4 (b)). The same phenomenon was found in PA6/mSEBS/OMMT blends and was ascribed to the interfacial tensions [25]. On the basis of the above analysis, the morphology evolution induced by migration and selective

localization of OMMT platelets in the representative nanocomposites prepared by two-step compounding with pre-mixed PET/OMMT was revealed and illustrated by the schematic drawing of Fig. 6.

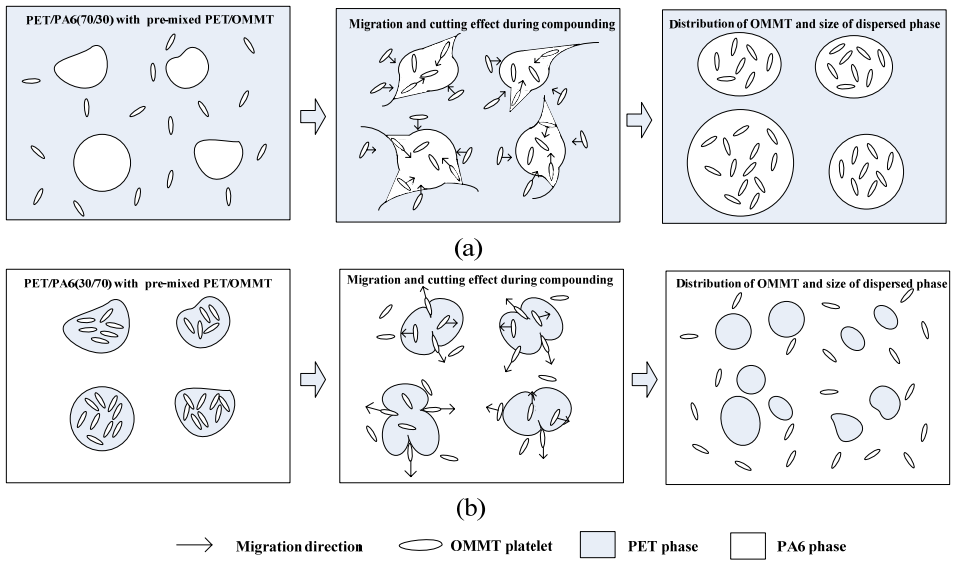

Fig.6 Schematic drawing of morphology evolution induced by migration and selective localization of OMMT platelets in the nanocomposites prepared by two-step with pre-mixed PET/OMMT: (a) PET/PA6(70/30) system, (b) PET/PA6(30/70) system

3.4 Mechanical property of the nanocomposites

To further study the effect of morphology on the performance of PET/PA6/OMMT nanocomposites, tensile test was carried out. Fig.7 shows the plots of tensile strength of nanocomposites prepared by different compounding processes versus OMMT content. It can be seen from Fig.7 (a) that the tensile strength of all samples of PET/PA6 (70/30) nanocomposites decreased with the increase of OMMT content, which might be attributed to the increased size of dispersed phase as shown in Fig.4 (a) [26,27]. At the same time, from Fig.7 (b) we can see that the varying trends in tensile strength of PET/PA6 (30/70) nanocomposites are complicated. For the non-migrating nanocomposites prepared by two-step compounding with pre-mixed PA6/OMMT, the tensile strength increased at first and then decreased with the increase of OMMT content (see line 3 in Fig.4 (b)), corresponding to the decreased size of dispersed phase at lower OMMT content and the increased size of that at higher OMMT content. But it is unexpected to see that tensile strength of nanocomposites prepared by one-step and two-step compounding with pre-mixed PET/OMMT, which had decreased size of dispersed phase, decreased as well. Comparing to that of the non-migrating nanocomposites, the decreased tensile strength of two migrating nanocomposites implies that migration cutting of OMMT during melt blending might has negative effect on the mechanical properties of polymer blends from another side, which may provide instructions for preparation of nanocomposites by filling layered nanoparticles into the immiscible polymer blends. From the above studies, we can conclude that the morphology, affected by the migration and selective localization of OMMT,

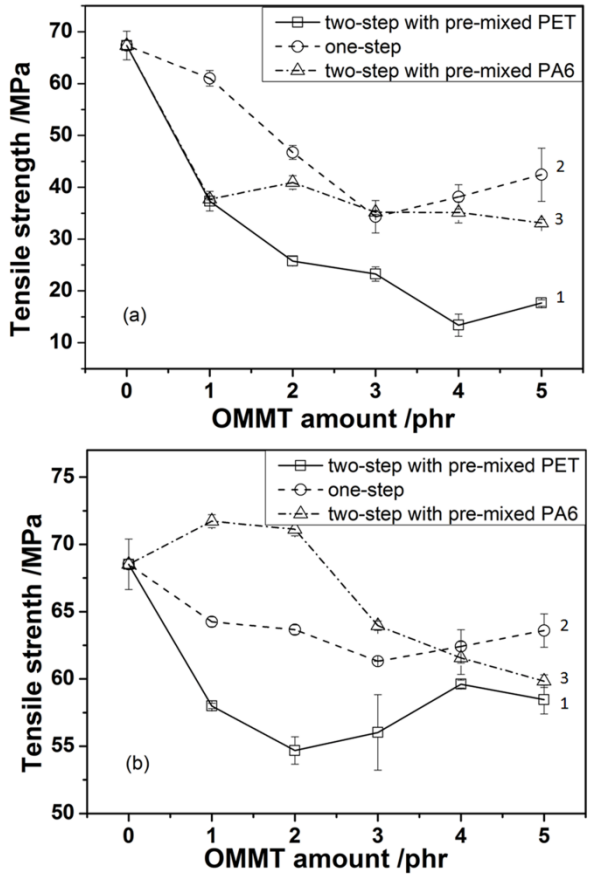

Fig.7 Plots of Tensile strength of nanocomposites prepared by different compounding sequences versus the amount of OMMT: (a) PET/PA6 (70/30) systems, (b) PET/PA6 (30/70) systems

had great influence on the final performance of the nanocomposites.

4 Conclusions

In this paper, PET/PA6/OMMT ternary blend was chosen as a representative nanocomposite to study the effect of migration and selective localization of layered nanoparticles on phase morphology of the nanocomposites prepared by melt compounding. The layered OMMT was incorporated into immiscible blends of PET/PA6 either by premixing in one of the blend components or by one-step blending. TEM showed the selective localization of the OMMT within PA6 phase independent of the blending procedures. It is demonstrated that OMMT platelets could be migrated from PET to PA6 phase. The migration and selective localization of OMMT could be attributed to the interfacial effects. While SEM observation and D_n analysis showed that the migration and selective localization of OMMT platelets had great effect on the morphology of the nanocomposites. For PET/PA6 (70/30) nanocomposites, the D_n of the dispersed PA6 phase increased with the increase of OMMT content. For the PET/PA6 (30/70) nanocomposites, the D_n of the dispersed PET phase decreased for nanocomposites prepared by one-step and two-step compounding with pre-mixed PET/OMMT. On the contrary, the D_n decreased at low OMMT content, and then increased very quickly for nanocomposites prepared by two-step compounding with pre-mixed PA6/OMMT. The conjunct action of migration cutting effect and viscosity effect played a role in the ultimate size of dispersed phase. The schematic of the migration and selective localization of OMMT (see Fig.6), as well as the evolution of phase morphology of nanocomposites can be inferred from the above analysis. Furthermore, the morphology of nanocomposites in turn affected the ultimate performance of the nanocomposites, as indicated by tensile test. It is deduced that performance of polymer blends could be tuned by changing compounding sequence and composition to control the migration of OMMT. We believe that this study on the processing, morphology and performance of PET/PA6/OMMT ternary blends provides a way to tune the phase morphology and performance of immiscible blend by layered nanoparticles and has the theoretical guidance to produce the high performance and functionalized nanocomposites.

Acknowledgements

The authors would like to acknowledge the financially supported from Natural Science Foundation of China (Grant: 51303032, 51473186, 51363002, 51173047, U1201243), the National Science and Technology Support Program (Grant: 2013BAC15B01), the Natural Science Foundation of Guangdong, China (Grants: 2012A090100006, 2013C2FC0009) and Special Funds of Guizhou Province Outstanding Young Scientists (Grant: (2013)20).

Notes

[a] *Key Laboratory for Polymeric Composite and Functional Materials of Ministry of Education, GDHPPC Lab, School of Chemistry and Chemical Engineering, Sun Yat-sen University, Guangzhou 510275, China*
[b] *National Engineering Research Center for Compounding and Modification of Polymer Materials, Guiyang 550014, China*
E-mail: cesrwh@mail.sysu.edu.cn.

References

1 Laura Gendre, James Njugun, Hrushikesh Abhyankar, Valentina Ermini. Materials & Design. 2015, 66, 486-491.
2 Lays B. Fitaroni, Juliana A. Lima, Sandra A. Cruz, Walter R. Waldman. Polymer Degradation and Stability. 2015, 111, 102-108.
3 Kesong Hu, Dhaval D. Kulkarni, Ikjun Choi, Vladimir V. Tsukruk. Progress in Polymer Science. 2014, 39, 1934-1972.
4 TianXiang Jin, Chuan Liu, Mi Zhou, Songgang Chai, Feng Chen, Qiang Fu. Composites Part A: Applied Science and Manufacturing. 2015, 68, 193-201.
5 Sebastien Livi, Gabriela Sar, Valeria Bugatti, Eliane Espuche, Jannick Duchet-Rumeau. RSC Advances. 2014, 4, 26452-26461.
6 Kidae Kwon and Jin-Hae Chang. Journal of Composite Materials. 2014, 12, 1-14.
7 Aravind Dasari, ZhongZhen Yu, YiuWing Mai. Polymer. 2005, 46, 5986-5991.
8 R. Scaffaro, L. Botta, M. C. Mistretta, F. P. La Mantia. eXPRESS Polymer Letters. 2013, 7, 873-884.
9 Mohamed Yousfi, Sophie Lepretre, Jeremie Soulestin, Bruno Vergnes, Marie-France Lacrampe, P. Krawczak. Journal Applied Polymer Science. 2014, 131, 1-10.
10 Razieh Mehrabi Kooshki, Ismail Ghasemi, Mohammad Karrabi, Hamed Azizi. Journal of Vinyl & Additive Technology. 2013, 5, 203-212.
11 Wei Yan, ShuHao Qin, JianBing Guo, MinMin Zhang, Min He, Jie Yu. Journal of Macromolecular Science, Part B: Physics. 2012, 51, 70-82.
12 Sumana Mallick, Anup K. Dhibar, B. B. Khatua. Journal of Applied Polymer Science. 2010, 116, 1010-1020.
13 Aravind Dasari, ZhongZhen Yu, MingShu Yang, QingXin Zhang, XiaoLin Xie, YiuWing Mai. Composites Science and Technology. 2006, 66, 3097-3114.
14 Dong Yan, Xiaofeng Li, Hui-Ling Ma, Xiu-Zhi Tang, Zhong Zhang, Zhong-Zhen Yu. Composites: Part A. 2013, 49, 35-41.
15 S. Gomari, I. Ghasemi, M. Karrabi,H. Azizi. Journal Polymer Research. 2012, 19, 9769-9780.
16 V. Prattipati, Y. S. Hu, S. Bandi, D. A. Schiraldi, A. Hiltner, E. Baer, S. Mehta. Journal of Applied Polymer Science. 2005, 97, 1361-1370.
17 Li Li, WenHong Ruan, MingQiu Zhang, MinZhi Rong. eXPRESS Polymer Letters. 2015, 9, 77-83.
18 Joung Sook Hong, Han Namkung, Kyung Hyun Ahn, Seung Jong Lee, Chong Youp Kim. Polymer. 2006, 47, 3967-3975.
19 XueBo Shi, ChunLei Wu, MinZhi Rong, Tibor Czigany, WenHong Ruan, MingQiu Zhang. Chinese Journal of Polymer Science. 2013, 31, 377-387.
20 P. G. de Gennes. The Journal of Chemical Physics. 1980, 72, 4756-4763
21 P. G. de Gennes. Macromolecules. 1981, 14, 1637-1644.
22 K. Binder. The Journal of Chemical Physics. 1983, 79, 6387-6409

23 Sumana Mallick, Prativa Kar, B. B. Khatua. Journal of Applied Polymer Science. 2012, 123, 1801-1811.
24 Yan Zhu, HaiYun Ma, LiFang Tong, ZhengPing Fang. Journal of Zhejiang University Science A. 2008, 11, 1614-1620.
25 I. Gonzalez, J.I. Eguiazabal, J. Nazabal. European Polymer Journal. 2006, 42, 2905-2913.
26 R. Scaffaro, L. Botta, M. C. Mistretta, F. P. La Mantia. eXPRESS Polymer Letters. 2013, 7, 873–884.
27 Mehdi Entezam, Hossein Ali Khonakdar, Ali Akbar Yousefi, Seyed Hassan Jafari, Udo Wagenknecht, Gert Heinrich. Materials and Design. 2013, 45, 110-117.